JGR Space Physics

RESEARCH ARTICLE
10.1029/2024JA032462

Fine Structure of Magnetospheric Magnetosonic Waves: 1. Elementary Rising-Tone Emissions Within Individual Harmonic

Jinxing Li[1], Jacob Bortnik[1], Sheng Tian[1], Qianli Ma[1,2], Xin An[3], Donglai Ma[1], Xiangning Chu[4], John Wygant[5], William S. Kurth[6], George B. Hospodarsky[6], Geoffrey D. Reeves[7], Herbert O. Funsten[8], Harlan Spence[9], and Daniel N. Baker[4]

[1]Department of Atmospheric and Oceanic Sciences, University of California, Los Angeles, CA, USA, [2]Center for Space Physics, Boston University, Boston, MA, USA, [3]Department of Earth, Planetary, and Space Sciences, University of California, Los Angeles, Los Angeles, CA, USA, [4]Laboratory for Atmospheric and Space Physics, University of Colorado Boulder, Boulder, CO, USA, [5]School of Physics and Astronomy, University of Minnesota, Minneapolis, MN, USA, [6]Department of Physics and Astronomy, University of Iowa, Iowa City, IA, USA, [7]Los Alamos National Laboratory, Space Science and Applications Group, Los Alamos, NM, USA, [8]Los Alamos National Laboratory, Los Alamos, NM, USA, [9]Institute for the Study of Earth, Oceans, and Space, University of New Hampshire, Durham, NH, USA

Key Points:

- Each harmonic of a magnetosonic wave may consist of a series of elementary rising-tone emissions
- The frequency sweep rate of elementary magnetosonic waves is likely proportional to the frequency
- Compound rising-tone magnetosonic waves consist of harmonics at the source, and gradually develop a continuous spectrum during propagation

Correspondence to:

J. Li,
jinxing.li.87@gmail.com

Citation:

Li, J., Bortnik, J., Tian, S., Ma, Q., An, X., Ma, D., et al. (2024). Fine structure of magnetospheric magnetosonic waves: 1. Elementary rising-tone emissions within individual harmonic. *Journal of Geophysical Research: Space Physics*, *129*, e2024JA032462. https://doi.org/10.1029/2024JA032462

Received 23 JAN 2024
Accepted 22 FEB 2024

Author Contributions:

Conceptualization: Jinxing Li, Jacob Bortnik
Data curation: Sheng Tian
Formal analysis: Jinxing Li
Methodology: Qianli Ma
Supervision: Jinxing Li, Jacob Bortnik
Writing – original draft: Jinxing Li
Writing – review & editing: Jacob Bortnik, Sheng Tian, Qianli Ma, Xin An, Donglai Ma, Xiangning Chu, John Wygant, William S. Kurth, George B. Hospodarsky, Geoffrey D. Reeves, Herbert O. Funsten, Harlan Spence, Daniel N. Baker

Abstract The present study uncovers the fine structures of magnetosonic waves by investigating the EFW waveforms measured by Van Allen Probes. We show that each harmonic of the magnetosonic wave may consist of a series of elementary rising-tone emissions, implying a nonlinear mechanism for the wave generation. By investigating an elementary rising-tone magnetosonic wave that spans a wide frequency range, we show that the frequency sweep rate is likely proportional to the wave frequency. We studied compound rising-tone magnetosonic waves, and found that they typically consist of multiple harmonics in the source region, and may gradually become continuous in frequency as they propagate away from source. Both elementary and compound rising-tone magnetosonic waves last for ∼1 min which is close to the bounce period of the ring proton distribution, but their relation is not fully understood.

Plain Language Summary Naturally occurring magnetosonic waves are a kind of electromagnetic wave in the Earth's magnetized space. Their frequency spectra typically exhibit a harmonic structure. Sometimes they exhibit a rising-tone feature, that is, the wave starts at a low pitch and gradually increases its frequency to a high pitch. Using the high-resolution data measured by Van Allen Probe satellites, the present study uncovers that each harmonic of a magnetosonic wave may have a fine structure: they consist of a series of elementary rising-tone emissions. The traditionally known rising-tone magnetosonic waves consist of multiple harmonics, and we name them "compound rising-tone magnetosonic waves". The compound rising-tone waves may gradually become continuous in spectrum as they propagate away from source. These findings give new insights to the generation of magnetosonic waves and their impact on space environment.

1. Introduction

Magnetosonic waves, also known as equatorial noises (Russell et al., 1970; Santolík et al., 2002) or ion Bernstein mode waves (Min & Liu, 2016), are ubiquitously observed in Earth's magnetosphere (Hrbáčková et al., 2015; Ma et al., 2013, 2016, 2019). Magnetosonic waves originate from proton ring distributions ($\partial f/\partial v_\perp > 0$, where f is the phase space density and $v_\perp$ is the proton perpendicular velocity) with the ring velocity comparable to the Alfven velocity (Chen et al., 2010, 2011; Curtis & Wu, 1979; Ma et al., 2014). They play an important role in radiation belt dynamics by accelerating energetic electrons via Landau resonance (Bortnik & Thorne, 2010; Horne et al., 2007), producing electron butterfly pitch angle distributions from ∼100 keV to several MeV both in the inner and outer radiation belts (Li, Ni, et al., 2016, Li, Bortnik, et al., 2016). Magnetosonic waves also interact with electrons via bounce resonance (Chen et al., 2015; Li et al., 2015; Shprits; 2016), which contributes to the formation of the electron butterfly distribution (Maldonado et al., 2016). Recent studies show magnetosonic wave modulation of energetic electrons in the dipolarization front, providing a new mechanism for electron energization therein (Fu et al., 2020).

Magnetosonic waves in Earth's magnetosphere exhibit different morphologies. It has been known that they typically consist of harmonics spaced at multiples of the proton gyrofrequency (f_{cp}) (Perraut et al., 1982; Santolík

et al., 2002), and the harmonic waves are coherent over a spatial scale of at least 3–5 wavelengths (Balikhin et al., 2015). Such a harmonic structure has been successfully explained by proton ring instabilities, which excite magnetosonic waves close to multiples of proton gyrofrequency at wave normal angles close to 90° (Balikhin et al., 2015; Chen et al., 2015; Min et al., 2018). Transfer function analysis and bicoherence analysis suggest that nonlinear interaction is negligible in the formation of the harmonic structure (Walker et al., 2020).

Magnetosonic waves sometimes exhibit periodic rising-tone features with a duration of ∼1 min, a repetition of a few minutes (Boardsen et al., 2014; Fu, Cao, Cully, et al., 2014; Fu, Cao, Zhima, et al., 2014) and a frequency sweep rate typically of ∼1 Hz/s. Magnetosonic waves occasionally consist of two series of periodic rising-tone waves known as "zipper-like" magnetosonic waves (Li et al., 2017). Burst mode waveform measured by Cluster satellites shows rising-tone magnetosonic waves that consist of multiple harmonics (Němec et al., 2015), and a case study suggests that the sweep rate maximizes at the equator (Walker et al., 2016). Van Allen Probe also observed the harmonic structure of rising-tone magnetosonic waves (Němec et al., 2020). These works investigated the magnetic field, plasma density and proton distribution variation in association with rising-tone magnetosonic waves, and no evidence of a modulation source has been clearly identified. Several hypotheses have been proposed to explain these rising-tone magnetosonic waves. By performing particle-in-cell simulations, Sun et al. (2020) indicated that the proton ring distribution excites magnetosonic waves at low frequencies in the beginning. As the waves scatter the ring distribution and lead to a new ring distribution at lower energies, magnetosonic waves are excited at higher frequencies, and this process occurs on a timescale comparable to observations.

Instruments with advanced capabilities are able to uncover phenomena that were previously hidden or invisible, leading to scientific discoveries or innovation. The recently released burst-mode waveforms measured by the EFW instrument onboard Van Allen Probes provides unprecedented opportunity for revealing fine structures of a variety of waves. In this paper, we report a new structure of magnetosonic waves, namely, the *elementary rising-tone* emissions within each harmonic. We also compare these elementary rising-tone magnetosonic waves with the traditionally known rising-tone ones, which we name as *compound rising-tone magnetosonic waves*, and discuss their possible origin.

2. Data Description

The Van Allen Probes (Mauk et al., 2013) were equipped with two instruments that measure electromagnetic waves with high cadence. The Waves instrument's Wave Form Receiver (WFR), a part of the Electric and Magnetic Field Instruments Suite and Integrated Science (EMFISIS) (Kletzing et al., 2013), provides survey-mode wave spectra over a frequency range of 10 Hz–12 kHz. It provides 3-D electric and magnetic waveform measurements at a cadence of 35,000 samples/s, and each episode of waveform data lasts for ∼6 s. Another instrument measuring waves is the Electric Field and Waves (EFW) instrument (Wygant et al., 2013), which consists of four deployable antennas that extend up to 100 m in space and two fixed antennas mounted on the spacecraft body. The EFW measures waveforms at cadences varying from 512 to 16,384 samples/s, and it provides continuous measurements of waveforms up to several hours, much longer than the 6-s WFR waveform. With high cadences and long durations, the EFW waveforms can produce unprecedented resolution in frequency, and thus are ideal for revealing the detailed structures of magnetosonic waves. This study also investigates proton distributions provided by the Helium Oxygen Proton Electron (HOPE) (Funsten et al., 2013; Spence et al., 2013) instruments to assist understanding the generation of magnetosonic waves.

3. Elementary Rising-Tone Emissions Embedded in Each Wave Harmonic

Figure 1 exhibits magnetosonic waves measured by Van Allen Probe A from 02:30 UT to 02:52 UT on 2 December 2015, when the satellite was in the pre-noon sector. Figure 1a shows the survey-mode magnetic spectrum measured by the WFR instrument. Figures 1b and 1c show the magnetic and electric spectra produced by Fast Fourier Transformation (FFT) of the EFW burst-mode waveforms. A window of 131,072 samples (8 s) and a shift window of 16,384 samples (1 s) were chosen for the FFT to optimize the frequency resolution (1/8 Hz) and temporal resolution. The EFW measurements show a harmonic structure above 19 f_{cp} (equatorial proton gyrofrequency). The wave normal angle (Figure 1d) and the ellipticity (Figure 1e) calculated using the Means (1972) method show that those harmonic waves were approximately perpendicularly propagating and linearly polarized, consistent with the essential characteristics of magnetosonic waves.

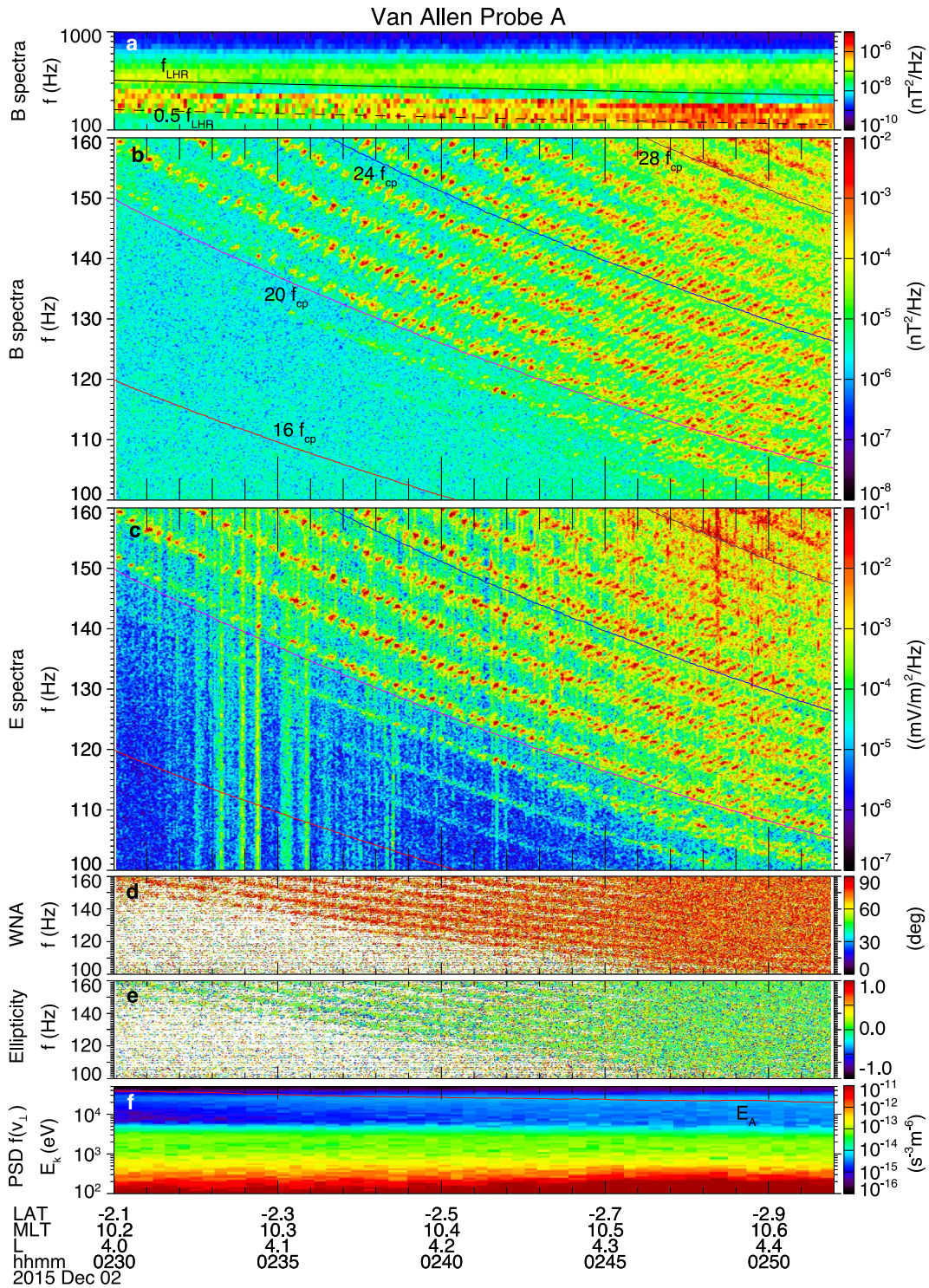

Figure 1. Van Allen Probe measurements during 02:30-02:52 UT on 2 December 2015. (a) The survey-mode magnetic spectrum measured by the WFR instrument (b)–(c) The magnetic and electric spectra derived from the EFW burst-mode waveforms by FFT. (d) The wave normal angle and (e) the ellipticity of waves calculated by Means (1972) method. (f) The perpendicular PSD of protons and the Alfven energy E_A.

The 20th–26th harmonics exhibit an internal fine structure, that is, each harmonic consists of a series of rising-tone emissions that has not been reported previously, to the best of our knowledge. These emissions grow from frequencies close to multiples of f_{cp}, and vanish before their frequencies rise to a higher harmonic. Each emission

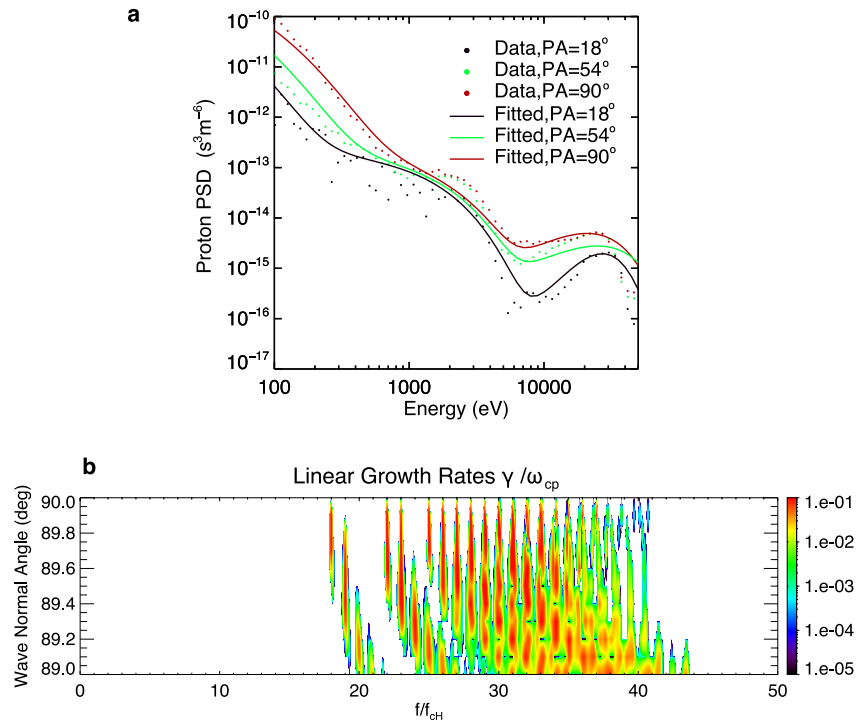

Figure 2. Wave linear growth calculation. (a) Proton PSD distribution measured by the HOPE instrument. (b) The calculated linear growth rate resulting from the interpolated proton PSD.

typically lasts for 30–70 s. The repetition period is about 18 s and does not vary over different harmonics. The temporal resolution of proton distribution measurements is 22 s, and is unable to resolve whether the proton distribution exhibits a periodic pattern. The frequency sweep rate is about 4 Hz/min and varies slightly over time.

The mechanism proposed by Sun et al. (2020) for compound rising-tone waves cannot explain the elementary magnetosonic waves, because the rising-tone structure is observed over all harmonics simultaneously. The discrete rising-tone emissions observed in each harmonic are somewhat analogous to the rising-tone emissions that make up chorus waves (Burtis & Helliwell, 1969). The excitation of chorus waves was believed to be associated with nonlinear interactions while different mechanisms have been proposed (e.g., Fu, Cao, Cully, et al., 2014; Omura et al., 2008; Tao et al., 2021). The rising-tone emissions in each magnetosonic wave harmonic imply a nonlinear excitation mechanism of those magnetosonic waves.

While the nonlinear excitation of these elementary rising-tone magnetosonic waves will be a future study, we apply the linear theory of wave growth for a basic understanding of their generation and spectral range. Figure 1f shows the perpendicular proton phase space density (PSD) derived from proton differential fluxes. Figure 2a shows the detailed perpendicular and parallel PSDs averaged over 02:45-02:50 UT, showing a ring distribution around 10–30 keV in both parallel and perpendicular directions. Assuming a nominal pitch angle range of [18°, 90°], the bounce periods of these ring protons (Lyons & Williams, 1984) are in the range of 33–87 s, which is very close to the durations of the elementary rising-tone emissions, but is significantly longer than their repetition period.

We use a combination of Gaussian and Kappa distributions to fit the proton PSD averaged from 02:45 UT to 02:50 UT. The averaged density provided by the EFW is 15 cm^{-3}, which is obtained by fitting the spacecraft potential to the density derived from the upper hybrid resonant frequency (Jahn et al., 2020; Kurth et al., 2015). Figure 2b shows the calculated linear wave growth rates (Kennel, 1966), demonstrating that magnetosonic waves can be readily generated at frequencies above 18 f_{cp}. The observation shows rising-tone emissions generally between n f_{cp} and ~(n + 1/2) f_{cp}, especially for harmonics from 20 f_{cp} to 30 f_{cp}. In contrast, the growth rates in Figure 2b show wave generation at frequencies centered around multiples of f_{cp}. The linear growth theory provides an explanation on the initial excitation of the wave harmonics, while the exact frequency range of each harmonic at saturation

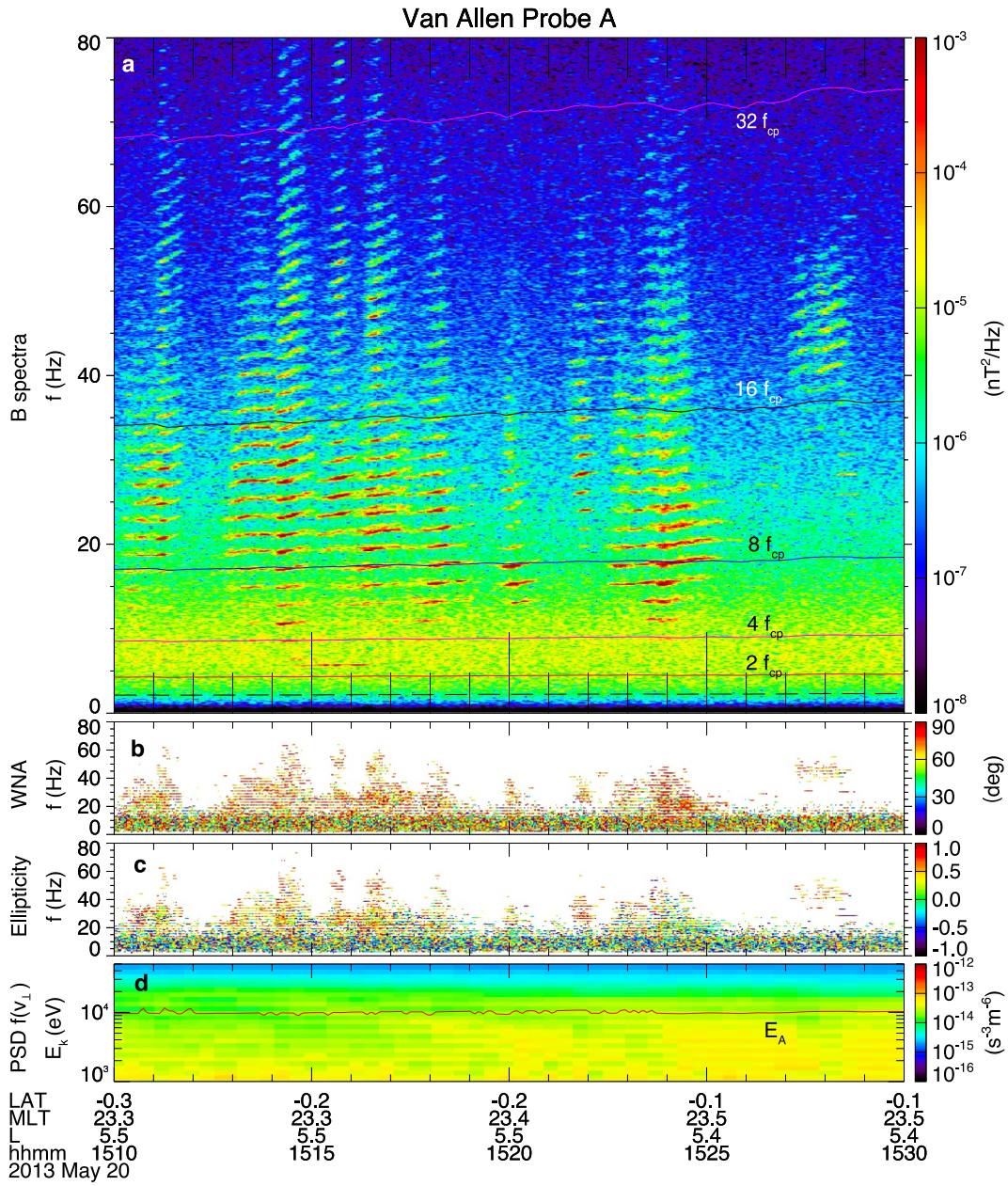

Figure 3. Elementary rising-tone magnetosonic waves observed on 20 May 2013. (a) The wave magnetic spectral intensity. (b) The wave normal angle and (c) the ellipticity. (d) The perpendicular PSD of protons.

amplitudes is not well captured, and a nonlinear mechanism for the rising-tone structure remains a topic for future studies.

Figure 3a shows another elementary rising-tone magnetosonic wave on 20 May 2012, in which the rising-tone feature is observed over a broad frequency range, from 4 f_{cp} to over f_{LHR}. These waves are perpendicularly propagating (Figure 3b), but they are right-hand polarized (Figure 3c), unlike most of magnetosonic waves. The proton ring distribution around 12 keV (Figure 3d) possibly supports the generation of these waves. These waves form a few series, and each series consists of elementary ring-tone emissions around multiples of f_{cp} which last for around 1 min. The frequency sweep rate is larger at higher frequencies, and is approximately proportional to their frequency. For instance, the waves observed between 15:14 UT and 15:15 UT show a frequency sweep rate of ~0.34 Hz/min at 8 f_{cp}, while it exhibits a sweep rate of ~0.80 Hz/min at 16 f_{cp}, and ~1.63 Hz/min at 32 f_{cp}. The

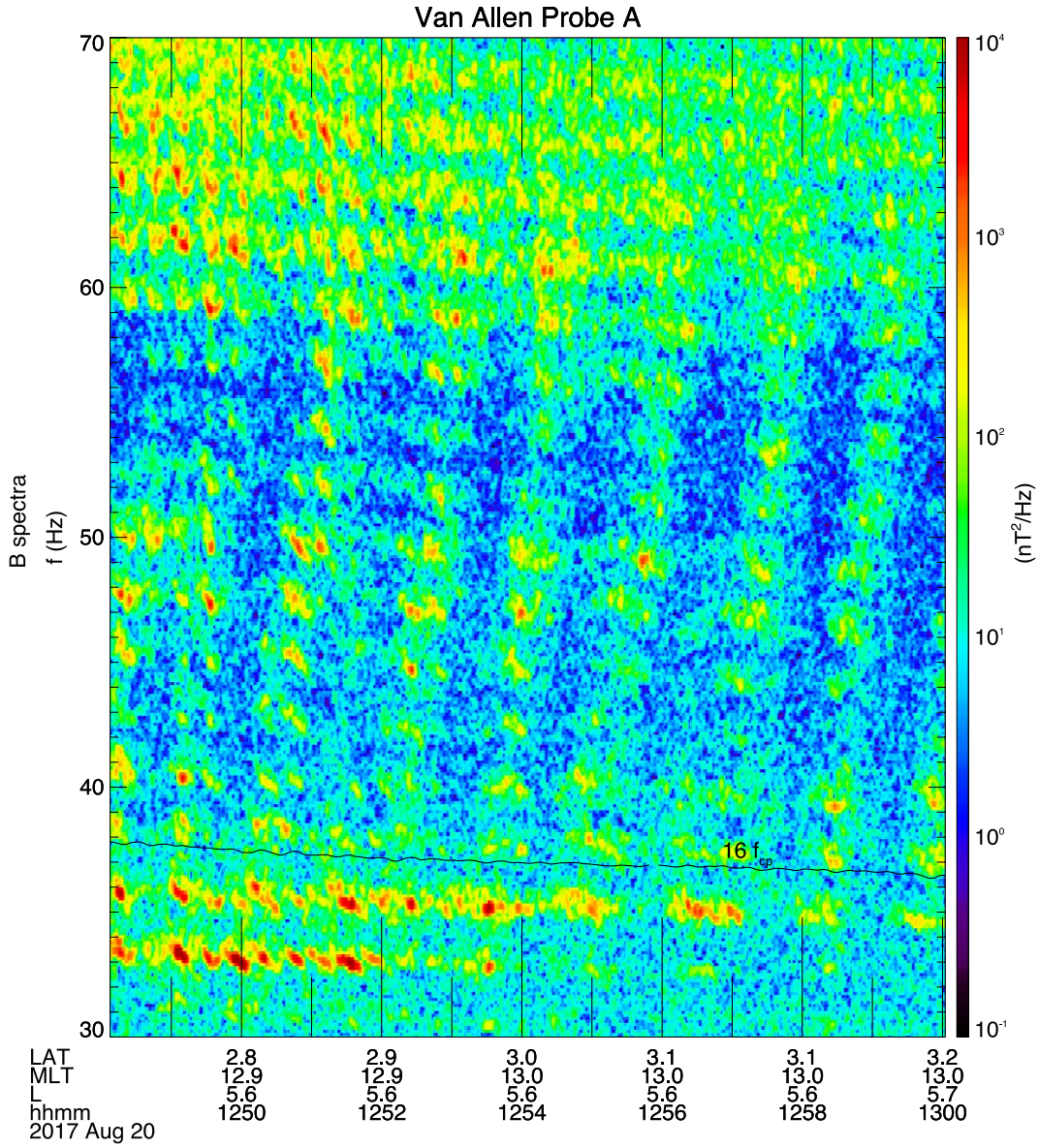

Figure 4. Observation of elementary falling-tone magnetosonic waves on 20 August 2017.

linearly increasing sweep rate is probably not associated with nonlinear harmonic effect (e.g., Huang et al., 2020), because the wave of 31 f_{cp} and other prime-number harmonics is obviously not the harmonic of waves at lower frequencies. Besides, the waves at 14 f_{cp} are more intense than the waves at 7 f_{cp}, and are not harmonics of waves at 7 f_{cp}. The mechanism that leads to a sweep rate that increases with wave frequency is yet to be understood. We note that these waves are not compound rising-tone waves because the harmonics of each series are observed almost simultaneously.

In addition to elementary rising-tone magnetosonic waves, the EFW instrument onboard the Van Allen Probe also recorded elementary falling-tone magnetosonic waves. Figure 4 shows Van Allen Probe A observations on 20 August 2017. A series of falling tone magnetosonic waves is observed from the 14th harmonic to the 29th harmonic. Between the 16th and the 25th harmonic, magnetosonic waves exhibit a periodic compound rising-tone structure. We note without delving into details that the falling tone sweep rate in this case is likely proportional to the harmonic number, like that in the rising-tone waves shown in Figure 3. The observation of falling-tone magnetosonic waves adds another interesting similarity between

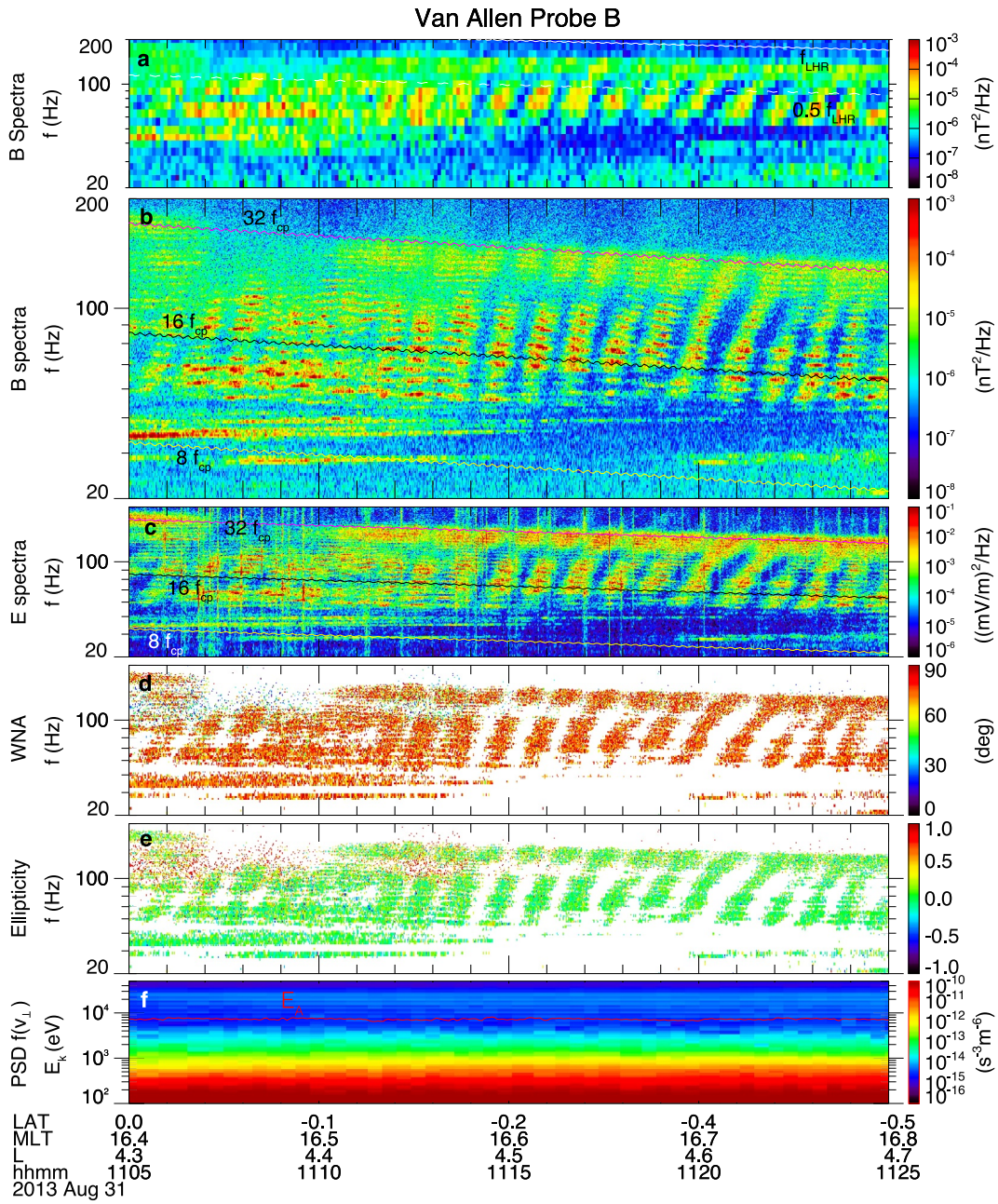

Figure 5. The same as in Figure 1 but showing compound rising-tone magnetosonic waves observed on 31 August 2013.

the morphologies of chorus waves and magnetosonic waves, providing additional insights into the wave-particle interaction.

4. Compound Rising-Tone Magnetosonic Waves Consisting of Harmonics

With the high resolution EFW data, we are able to investigate whether compound rising-tone magnetosonic waves can intrinsically be decomposed into multiple harmonics. Figure 5a shows the WFR survey-mode magnetic spectra measured on 31 August 2013. Periodic rising-tone magnetosonic waves were observed between 11:12 UT and 11:25 UT. The EFW burst-mode wave magnetic and electric spectra, shown in Figures 5b and 5c, clearly indicate that each of those rising-tone emissions consists of multiple harmonics. The compound

rising-tone magnetosonic waves are perpendicularly propagating and linearly polarized (Figures 5d and 5e). They are observed at multiples of f_{cp}, suggesting that those magnetosonic waves are likely locally generated. A proton ring structure in PSD is seen just above the Alfven energy (Figure 5f), consistent with a local generation mechanism.

We note that the waveform sampling rate for this case is 1,024 samples/s, much lower than the case shown in Figure 1. Hence, the data is unable to reveal fine structures inside each harmonic if any. The periodicity is about 1 min, and each group lasts for about 1.6 min, close to the bounce period of ring protons that excite those waves. While these compound rising-tone magnetosonic waves have similar temporal scales to elementary rising-tone waves, their sweep rate is about 70 Hz/min, much higher than that of elementary ones. Our detailed study shows that these periodic occurring of compounding rising-tone waves are not modulated by magnetic field, plasma density, or energetic proton distribution, consistent with previous studies (e.g., Boardsen et al., 2014; Fu, Cao, Zhima, et al., 2014; Němec et al., 2020).

Figure 6 shows a different event recorded by Van Allen Probe A on 12 December 2012. Again, we show WFR survey-mode spectra (Figure 6a) and EFW burst-mode spectra (Figures 6b and 6c) for a comparison. The wave normal angle (Figure 6d) and the ellipticity (Figure 6e) indicate that all the waves shown in this figure are magnetosonic waves. The EFW sampling rate is 512 samples/s for this case and is not sufficient to resolve the possible elementary rising-tone structure.

Rising-tone magnetosonic waves are seen above 120 Hz. They show a clear harmonic structure from 13:30 UT to 13:50 with a frequency gap between adjacent harmonics of about 8 Hz, which slowly increases over time. Assuming a dipole background magnetic field, the estimated source region of those waves, based on generation at harmonics of the local f_{cp}, is at $L = 3.9$. The harmonic structure was clear when the satellite was at $L = 3.7$–4.2, possibly close to the source. At earlier times, as the satellite approached large L shells, the harmonics gradually vanished, the wave intensities became weaker, and the spectra became continuous over frequency. One possibility could be that the waves were generated with the same periodicity in the source region that spanned a certain area. At locations farther from the source, waves from a broad source region mix together, resulting in a continuous rising-tone spectrum. Another possible mechanism could be the spectral broadening effect due to self-phase modulation. This effect occurs when a short pulse travels through a medium with varying reflective index, which produce a phase shift, leading to the change of the pulse's spectrum (Stolen & Lin, 1978). The periodicity of these rising-tone magnetosonic waves is ∼1.4 min and is unchanged during the propagation, while the frequency sweep rate slightly increased from ∼160 Hz at $L = 3.9$–∼180 Hz/min at $L = 4.6$.

5. Conclusions

This paper uncovers the elementary rising-tone structure of magnetosonic waves in Earth's magnetosphere, which is only plausible using the recently released burst-mode waveform measurements by the EFW instrument onboard Van Allen Probes. We summarize the new findings as follows.

1. Magnetosonic waves have fine structures within the harmonics, that is, each harmonic may consist of a series of elementary rising-tone emissions. This suggests a nonlinear excitation of magnetosonic waves.
2. A case study shows that the frequency sweep rate of the elementary rising-tone magnetosonic wave is likely proportional to the wave frequency.
3. Elementary falling-tone magnetosonic waves are also recorded. The periodicity is close to that of elementary rising-tone waves.
4. Compound rising-tone magnetosonic waves typically exhibit harmonic structures in the source region, and may gradually develop a continuous spectrum over frequency as they propagate further away from the source. The elementary and compound rising-tone magnetosonic waves have similar durations of about 1 min, which is close to the bounce period of the ring protons. The relation between the two rising-tone structures is yet to be understood.

The fine structures we uncover in this paper provide new insights into the complex nature of magnetosonic waves and their generation mechanism as well as their impact on ring current ions and electrons. In the future, we plan to

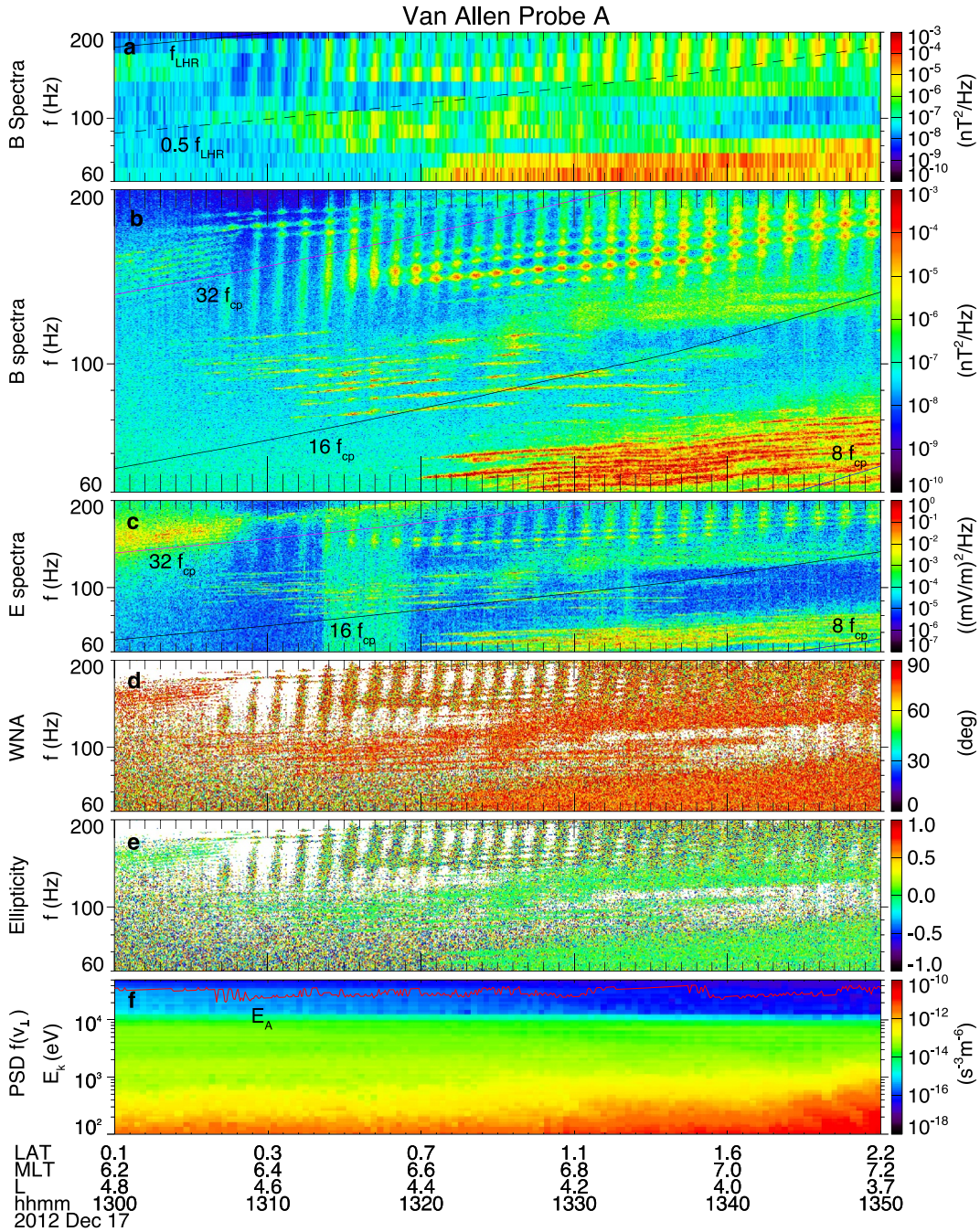

Figure 6. The same as in Figure 5, showing an observation of non-local magnetosonic waves measured on 17 December 2012.

carry out a statistical study with all available EFW data to explore under what favorable conditions and in what regions elementary rising-tone MS waves are typically observed.

Data Availability Statement

The Van Allen Probe data analysis is carried out using the SPEDAS v4.1 software (Angelopoulos et al., 2019), which is publicly available at (SPEDAS, 2023). The proton distributions measured by the HOPE instrument are

publicly available from (Funsten, 2022). The EFW waveform and the derived plasma density data are publicly available from (EFW, 2022). The magnetic field (Kletzing, 2022) and EMFISIS wave data (Kletzing & Smith, 2022) are publicly available.

Acknowledgments
JL, JB and XA acknowledge NASA Grants LWS- 80NSSC20K0201. JL and JB acknowledge NASA Grants 80NSSC21K0522, 80NSSC18K1227, and NNX14AI18G, and the Grant DE-SC0010578. XA and JB acknowledge the NASA Grant 80NSSC20K0917. QM acknowledges the NASA Grant 80NSSC20K0196 and NSF Grant AGS-2225445. This work is supported by RBSP-ECT and EMFISIS funding provided by JHU/APL contract No. 967399 and 921647 under NASA's prime contract No. NAS5-01072. This paper is dedicated to the memory of the late Craig Kletzing who passed on 10 August 2023. Craig served as the Principal Investigator of the Van Allen Probe EMFISIS Suite and contributed to over 30 space missions throughout his career.

References

Angelopoulos, V., Cruce, P., Drozdov, A., Grimes, E. W., Hatzigeorgiu, N., King, D. A., et al. (2019). The space physics environment data analysis system (SPEDAS). *Space Science Reviews*, *215*(1), 9. Space Science Reviews - Springer. https://doi.org/10.1007/s11214-018-0576-4

Balikhin, M. A., Shprits, Y. Y., Walker, S. N., Chen, L., Cornilleau-Wehrlin, N., Dandouras, I., et al. (2015). Observations of discrete harmonics emerging from equatorial noise. *Nature Communications*, *6*(1), 7703. https://doi.org/10.1038/ncomms8703

Boardsen, S. A., Hospodarsky, G. B., Kletzing, C. A., Pfaff, R. F., Kurth, W. S., Wygant, J. R., & MacDonald, E. A. (2014). Van Allen Probe observations of periodic rising frequencies of the fast magnetosonic mode. *Geophysical Research Letters*, *41*(23), 8161–8168. https://doi.org/10.1002/2014GL062020

Bortnik, J., & Thorne, R. M. (2010). Transit time scattering of energetic electrons due to equatorially confined magnetosonic waves. *Journal of Geophysical Research*, *115*(A7), A07213. https://doi.org/10.1029/2010JA015283

Burtis, W. J., & Helliwell, R. A. (1969). Banded chorus—A new type of VLF radiation observed in the magnetosphere by OGO 1 and OGO 3. *Journal of Geophysical Research*, *74*(11), 3002–3010. https://doi.org/10.1029/JA074i011p03002

Chen, L. (2015). Wave normal angle and frequency characteristics of magnetosonic wave linear instability. *Geophysical Research Letters*, *42*(12), 4709–4715. https://doi.org/10.1002/2015GL064237

Chen, L., Maldonado, A., Bortnik, J., Thorne, R. M., Li, J., Dai, L., & Zhan, X. (2015). Nonlinear bounce resonances between magnetosonic waves and equatorially mirroring electrons. *Journal of Geophysical Research: Space Physics*, *120*(8), 6514–6527. https://doi.org/10.1002/2015JA021174

Chen, L., Thorne, R. M., Jordanova, V. K., & Horne, R. B. (2010). Global simulation of magnetosonic wave instability in the storm time magnetosphere. *Journal of Geophysical Research*, *115*(A11), A11222. https://doi.org/10.1029/2010JA015707

Chen, L., Thorne, R. M., Jordanova, V. K., Thomsen, M. F., & Horne, R. B. (2011). Magnetosonic wave instability analysis for proton ring distributions observed by the LANL magnetospheric plasma analyzer. *Journal of Geophysical Research*, *116*(A3), A03223. https://doi.org/10.1029/2010JA016068

Curtis, S., & Wu, C. (1979). Gyroharmonic emissions induced by energetic ions in the equatorial plasmasphere. *Journal of Geophysical Research*, *84*(A6), 2597–2607. https://doi.org/10.1029/JA084iA06p02597

EFW. (2022). Van allen Probe EFW data [Dataset]. *EFW*. Retrieved from https://rbsp.space.umn.edu/rbsp_efw/

Fu, H. S., Cao, J. B., Cully, C. M., Khotyaintsev, Y. V., Vaivads, A., Angelopoulos, V., et al. (2014). Whistler-mode waves inside flux pileup region: Structured or unstructured? *Journal of Geophysical Research: Space Physics*, *119*(11), 9089–9100. https://doi.org/10.1002/2014JA020204

Fu, H. S., Cao, J. B., Zhima, Z., Khotyaintsev, Y. V., Angelopoulos, V., Santolík, O., et al. (2014). First observation of rising-tone magnetosonic waves. *Geophysical Research Letters*, *41*(21), 7419–7426. https://doi.org/10.1002/2014GL061867

Fu, H. S., Zhao, M. J., Yu, Y., & Wang, Z. (2020). A new theory for energetic electron generation behind dipolarization front. *Geophysical Research Letters*, *47*, e2019GL086790. https://doi.org/10.1029/2019GL086790

Funsten, H. O. (2022). Van allen Probe A energetic particle, composition, and thermal plasma suite (ECT) Helium oxygen proton electron, HOPE, mass spectrometer pitch angle resolved science data. Electron fluxes, 15 eV to 50 keV, and ion fluxes, 1 eV to 50 keV, as measured in alternate spin cadence, level 3, release #4 (L3), 11.35 s data [Dataset]. *NASA Space Physics Data Facility*. https://doi.org/10.48322/17p9-rf75

Funsten, H. O., Skoug, R. M., Guthrie, A. A., MacDonald, E. A., Baldonado, J. R., Harper, R. W., et al. (2013). Helium, oxygen, proton, and electron (HOPE) mass spectrometer for the Radiation Belt Storm Probes mission. *Space Science Reviews*, *179*(1–4), 423–484. https://doi.org/10.1007/s11214-013-9968-7

Horne, R. B., Thorne, R. M., Glauert, S. A., Meredith, N. P., Pokhotelov, D., & Santolik, O. (2007). Electron acceleration in the Van Allen radiation belts by fast magnetosonic waves. *Geophysical Research Letters*, *34*(17), L17107. https://doi.org/10.1029/2007GL030267

Hrbáčková, Z., Santolík, O., Němec, F., Macúšová, E., & Cornilleau-Wehrlin, N. (2015). Systematic analysis of occurrence of equatorial noise emissions using 10 years of data from the Cluster mission. *Journal of Geophysical Research: Space Physics*, *120*(2), 1007–1021. https://doi.org/10.1002/2014JA020268

Huang, S. Y., Deng, D., Yuan, Z. G., Jiang, K., Li, J. X., Deng, X. H., et al. (2020). First observations of magnetosonic waves with nonlinear harmonics. *Journal of Geophysical Research: Space Physics*, *125*(6), e2019JA027724. https://doi.org/10.1029/2019JA027724

Jahn, J.-M., Goldstein, J., Kurth, W. S., Thaller, S., De Pascuale, S., Wygant, J., et al. (2020). Determining plasmaspheric density from the upper hybrid resonance and from the spacecraft potential: How do they compare? *Journal of Geophysical Research: Space Physics*, *125*(3), e2019JA026860. https://doi.org/10.1029/2019JA026860

Kennel, C. (1966). Low-frequency whistler mode. *Physics of Fluids*, *9*(11), 2190–2202. https://doi.org/10.1063/1.1761588

Kletzing, C., Kurth, W. S., Acuna, M., MacDowall, R. J., Torbert, R. B., Averkamp, T., et al. (2013). The electric and magnetic field instrument suite and integrated science (EMFISIS) on RBSP. *Space Science Reviews*, *179*(1–4), 127–181. https://doi.org/10.1007/s11214-013-9993-6

Kletzing, C. A. (2022). Van allen Probe A fluxgate magnetometer 4 second resolution data in SM coordinates [Dataset]. *NASA Space Physics Data Facility*. https://doi.org/10.48322/d15r-3a05

Kletzing, C. A., & Smith, C. W. (2022). Van allen Probe A electric and magnetic field instrument suite and integrated science (EMFISIS) waveform receiver (WFR) cross spectral matrix, level 2 (L2), 6 s data [Dataset]. *NASA Space Physics Data Facility*. https://doi.org/10.48322/be1v-n754

Kurth, W. S., De Pascuale, S., Faden, J. B., Kletzing, C. A., Hospodarsky, G. B., Thaller, S., & Wygant, J. R. (2015). Electron densities inferred from plasma wave spectra obtained by the Waves instrument on Van Allen Probes. *Journal of Geophysical Research: Space Physics*, *120*(2), 904–914. https://doi.org/10.1002/2014JA020857

Li, J., Bortnik, J., Li, W., Ma, Q., Thorne, R. M., Kletzing, C. A., et al. (2017). "Zipper-like" periodic magnetosonic waves: Van Allen Probes, THEMIS, and magnetospheric multiscale observations. *Journal of Geophysical Research: Space Physics*, *122*(2), 1600–1610. https://doi.org/10.1002/2016JA023536

Li, J., Bortnik, J., Thorne, R. M., Li, W., Ma, Q., Baker, D. N., et al. (2016). Ultrarelativistic electron butterfly distributions created by parallel acceleration due to magnetosonic waves. *Journal of Geophysical Research: Space Physics*, *121*(4), 3212–3222. https://doi.org/10.1002/2016JA022370

Li, J., Ni, B., Ma, Q., Xie, L., Pu, Z., Fu, S., et al. (2016). Formation of energetic electron butterfly distributions by magnetosonic waves via Landau resonance. *Geophysical Research Letters*, *43*(7), 3009–3016. https://doi.org/10.1002/2016GL067853

Li, X., Tao, X., Lu, Q., & Dai, L. (2015). Bounce resonance diffusion coefficients for spatially confined waves. *Geophysical Research Letters*, *42*(22), 9591–9599. https://doi.org/10.1002/2015GL066324

Lyons, L. R., & Williams, D. J. (1984). *Quantitative aspects of magnetospheric physics*. D. Reidel Co. https://doi.org/10.1007/978-94-017-2819-5

Ma, Q., Li, W., Bortnik, J., Kletzing, C. A., Kurth, W. S., Hospodarsky, G. B., & Wygant, J. R. (2019). Global survey and empirical model of fast magnetosonic waves over their full frequency range in earth's inner magnetosphere. *Journal of Geophysical Research: Space Physics*, *124*(12), 270–282. https://doi.org/10.1029/2019JA027407

Ma, Q., Li, W., Chen, L., Thorne, R. M., & Angelopoulos, V. (2014). Magnetosonic wave excitation by ion ring distribution in the Earth's inner magnetosphere. *Journal of Geophysical Research: Space Physics*, *119*(2), 844–852. https://doi.org/10.1002/2013JA019591

Ma, Q., Li, W., Thorne, R. M., & Angelopoulos, V. (2013). Global distribution of equatorial magnetosonic waves observed by THEMIS. *Geophysical Research Letters*, *40*(10), 1895–1901. https://doi.org/10.1002/grl.50434

Ma, Q., Li, W., Thorne, R. M., Bortnik, J., Kletzing, C. A., Kurth, W. S., & Hospodarsky, G. B. (2016). Electron scattering by magnetosonic waves in the inner magnetosphere. *Journal of Geophysical Research: Space Physics*, *121*(1), 274–285. https://doi.org/10.1002/2015JA021992

Maldonado, A. A., Chen, L., Claudepierre, S. G., Bortnik, J., Thorne, R. M., & Spence, H. (2016). Electron butterfly distribution modulation by magnetosonic waves. *Geophysical Research Letters*, *43*(7), 3051–3059. https://doi.org/10.1002/2016GL068161

Mauk, B. H., Fox, N. J., Kanekal, S. G., Kessel, R. L., Sibeck, D. G., & Ukhorskiy, A. (2013). Science objectives and rationale for the radiation BeltStorm Probes mission. *Space Science Reviews*, *179*(1–4), 3–27. https://doi.org/10.1007/s11214-012-9908-y

Means, J. D. (1972). Use of the three-dimensional covariance matrix in analyzing the polarization properties of plane waves. *Journal of Geophysical Research*, *77*(28), 5551–5559. https://doi.org/10.1029/JA077i028p05551

Min, K., & Liu, K. (2016). Understanding the growth rate patterns of ion Bernstein instabilities driven by ring-like proton velocity distributions. *Journal of Geophysical Research: Space Physics*, *121*(4), 3036–3049. https://doi.org/10.1002/2016JA022524

Min, K., Liu, K., Wang, X., Chen, L., & Denton, R. E. (2018). Fast magnetosonic waves observed by Van Allen Probes: Testing local wave excitation mechanism. *Journal of Geophysical Research: Space Physics*, *123*(1), 497–512. https://doi.org/10.1002/2017JA024867

Němec, F., Santolík, O., Hrbáčková, Z., Pickett, J. S., & Cornilleau-Wehrlin, N. (2015). Equatorial noise emissions with quasiperiodic modulation of wave intensity. *Journal of Geophysical Research: Space Physics*, *120*(4), 2649–2661. https://doi.org/10.1002/2014JA020816

Němec, F., Tomori, A., Santolík, O., Boardsen, S. A., Hospodarsky, G. B., Kurth, W. S., et al. (2020). Fine harmonic structure of equatorial noise with a quasiperiodic modulation. *Journal of Geophysical Research: Space Physics*, *125*(3), e2019JA027509. https://doi.org/10.1029/2019JA027509

Omura, Y., Katoh, Y., & Summers, D. (2008). Theory and simulation of the generation of whistler-mode chorus. *Journal of Geophysical Research*, *113*(A4), A04223. https://doi.org/10.1029/2007JA012622

Perraut, S., Roux, A., Robert, P., Gendrin, R., Sauvaud, J.-A., Bosqued, J.-M., et al. (1982). A systematic study of ULF waves above FH+ from GEOS 1 and 2 measurements and their relationships with proton ring distributions. *Journal of Geophysical Research*, *87*(A8), 6219–6236. https://doi.org/10.1029/JA087iA08p06219

Russell, C. T., Holzer, R. E., & Smith, E. J. (1970). OGO 3 observations of ELF noise in the magnetosphere: 2. The nature of the equatorial noise. *Journal of Geophysical Research*, *75*(4), 755–768. https://doi.org/10.1029/JA075i004p00755

Santolík, O., Pickett, J. S., Gurnett, D. A., Maksimovic, M., & Cornilleau-Wehrlin, N. (2002). Spatiotemporal variability and propagation of equatorial noise observed by Cluster. *Journal of Geophysical Research*, *107*(A12), 1495. https://doi.org/10.1029/2001JA009159

Shprits, Y. Y. (2016). Estimation of bounce resonant scattering by fast magnetosonic waves. *Geophysical Research Letters*, *43*(3), 998–1006. https://doi.org/10.1002/2015GL066796

SPEDAS. (2023). Space physics environment data analysis software [Software]. *SPEDAS*. Retrieved from http://spedas.org/wiki/index.php?title=Downloads_and_Installation

Spence, H. E., Reeves, G. D., Baker, D. N., B Blake, J., Bolton, M., Bourdarie, S., et al. (2013). Science goals and overview of the energetic particle, composition, and thermal plasma (ECT) suite on NASA's radiation belt storm Probes (RBSP) mission. *Space Science Reviews*, *179*(1–4), 311–336. https://doi.org/10.1007/s11214-013-0007-5

Stolen, R. H., & Lin, Q. (1978). Self-phase-modulation in silica optical fibers. *Physical Review A*, *17*(4), 1448–1453. https://doi.org/10.1103/PhysRevA.17.1448

Sun, J., Chen, L., Wang, X., Boardsen, S., Lin, Y., & Xia, Z. (2020). Particle-in-cell simulation of rising-tone magnetosonic waves. *Geophysical Research Letters*, *47*(18), e2020GL089671. https://doi.org/10.1029/2020GL089671

Tao, X., Zonca, F., & Chen, L. (2021). A "Trap-Release-Amplify" model of chorus waves. *Journal of Geophysical Research: Space Physics*, *126*(9), e2021JA029585. https://doi.org/10.1029/2021JA029585

Walker, S. N., Balikhin, M. A., Yearby, K. H., & Aryan, H. (2020). Equatorial magnetosonic waves: Do nonlinear interactions play a role in their evolution? *Journal of Geophysical Research: Space Physics*, *125*(1), e2019JA027572. https://doi.org/10.1029/2019JA027572

Walker, S. N., Demekhov, A. G., Boardsen, S. A., Ganushkina, N. Y., Sibeck, D. G., & Balikhin, M. A. (2016). Cluster observations of non–time continuous magnetosonic waves. *Journal of Geophysical Research: Space Physics*, *121*(10), 9701–9716. https://doi.org/10.1002/2016JA023287

Wygant, J. R., Bonnell, J. W., Goetz, K., Ergun, R. E., Mozer, F. S., Bale, S. D., et al. (2013). The electric field and waves instrument on the Radiation Belt Storm Probes mission. *Space Science Reviews*, *179*(1–4), 183–220. https://doi.org/10.1007/s11214-013-0013-7